Climate of the Past

Open Access

Constraining Holocene hydrological changes in the Carpathian–Balkan region using speleothem $\delta^{18}O$ and pollen-based temperature reconstructions

V. Drăguşin[1,2,3], **M. Staubwasser**[3], **D. L. Hoffmann**[4], **V. Ersek**[5,6], **B. P. Onac**[7,8], **and D. Veres**[8]

[1]Emil Racoviţă Institute of Speleology, Romanian Academy, Frumoasă 31, 010986, Bucharest, Romania
[2]Department of Geology, Babeş-Bolyai University, Kogălniceanu 1, 400084, Cluj-Napoca, Romania
[3]Institute of Geology and Mineralogy, University of Cologne, Greinstrasse 4–6, 50939, Cologne, Germany
[4]National Research Centre for Human Evolution, Paseo Sierra de Atapuerca, s/n, 09002 Burgos, Spain
[5]Department of Geography, Northumbria University, Ellison Building, NE1 8ST, Newcastle upon Tyne, UK
[6]Department of Earth Sciences, University of Oxford, South Parks Rd, OX1 3AN, Oxford, UK
[7]School of Geosciences, University of South Florida, 4202 E. Fowler Ave., NES 107, FL 33620, Tampa, USA
[8]Institute of Speleology, Romanian Academy, Clinicilor 5, 400006, Cluj-Napoca, Romania

Correspondence to: M. Staubwasser (m.staubwasser@uni-koeln.de)

Abstract. Here we present a speleothem isotope record (POM2) from Ascunsă Cave (Romania) that provides new data on past climate changes in the Carpathian–Balkan region from 8.2 ka until the present. This paper describes an approach to constrain the effect of temperature changes on calcite $\delta^{18}O$ values in stalagmite POM2 over the course of the middle Holocene (6–4 ka), and across the 8.2 and 3.2 ka rapid climate change events. Independent pollen temperature reconstructions are used to this purpose. The approach combines the temperature-dependent isotope fractionation of rain water during condensation and fractionation resulting from calcite precipitation at the given cave temperature. The only prior assumptions are that pollen-derived average annual temperature reflects average cave temperature, and that pollen-derived coldest and warmest month temperatures reflect the range of condensation temperatures of rain above the cave site. This approach constrains a range of values between which speleothem $\delta^{18}O$ changes should be found if controlled only by surface temperature variations at the cave site. Deviations of the change in $\delta^{18}O_{c\_spel}$ values from the calculated temperature-constrained range of change are interpreted towards large-scale variability of climate–hydrology.

Following this approach, we show that an additional $\sim 0.6\,‰$ enrichment of $\delta^{18}O_c$ in the POM2 stalagmite was caused by changing hydrological patterns in SW Romania across the middle Holocene, most likely comprising local evaporation from the soil and an increase in Mediterranean moisture $\delta^{18}O$. Further, by extending the calculations to other speleothem records from around the entire Mediterranean basin, it appears that all eastern Mediterranean speleothems recorded a similar isotopic enrichment due to changing hydrology, whereas all changes recorded in speleothems from the western Mediterranean are fully explained by temperature variation alone. This highlights a different hydrological evolution between the two sides of the Mediterranean.

Our results also demonstrate that during the 8.2 ka event, POM2 stable isotope data essentially fit the temperature-constrained isotopic variability. In the case of the 3.2 ka event, an additional climate-related hydrological factor is more evident. This implies a different rainfall pattern in the Southern Carpathian region during this event at the end of the Bronze Age.
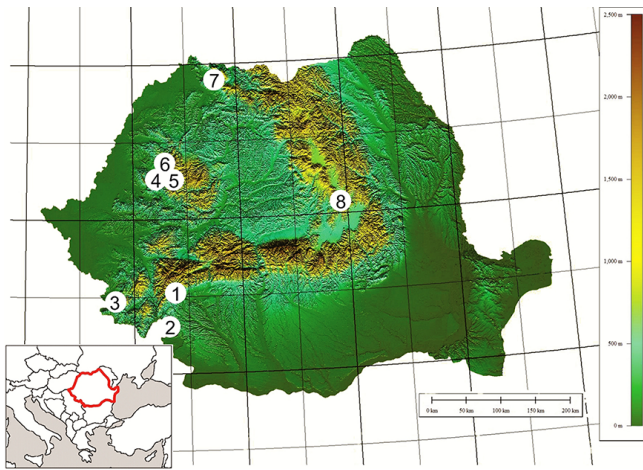
Figure 1. Location of Romanian palaeoclimate records and meteorological stations mentioned in the text: 1 – Ascunsă Cave; 2 – Drobeta meteorological station; 3 – Poleva Cave; 4 – Urşilor Cave; 5 – V11 Cave; 6 – Stâna de Vale meteorological station; 7 – Steregoiu peat bog; 8 – Sfânta Ana Lake.

1 Introduction

In the region surrounding the eastern Mediterranean, proxy records suggest that conditions were more humid during the early Holocene compared to present-day moisture budgets (Rossignol-Strick, 1999; Rohling et al., 2002). Enhanced freshwater flux roughly between 10 000 years before present (10 ka) and 6 ka led to stratification and sapropel formation in the eastern Mediterranean. At the same time, depleted δ^{18}O values in lacustrine calcareous microfossils and endogenic carbonate deposits suggest less evaporation across the region during that time compared to the present day. A stacked oxygen isotope record generated from lake proxies around the eastern Mediterranean shows a general drying trend between 6 and 4 ka (Roberts et al., 2008). A pattern of increasing δ^{18}O values with time from the early to mid-late Holocene is documented in speleothem records from south-central Europe and the eastern Mediterranean (McDermott et al., 2011, and references therein). This has been suggested by McDermott et al. (2011) to reflect more efficient rainout from an Atlantic source of moisture and less of it reaching the eastern Mediterranean region during the late Holocene.

Due to the topographic complexity and rather sparse data distribution, reports from across the Carpathian–Balkan region do not provide yet a common view on past environmental change, but rather point to possibly contrasting Holocene hydroclimatic evolution at the regional scale (Feurdean et al., 2008; Magyari et al., 2013). Lake records from the southern Balkans, such as Ioannina, Greece (Frogley et al., 2001), and Prespa and Ohrid, Macedonia (Leng et al., 2010) indicate high humidity throughout the early Holocene, whereas palaeolimnological records from Steregoiu, NW Romania (Feurdean et al., 2007) and Sfânta Ana, central Romania (Magyari

et al., 2009), suggest that lower humidity persisted in the area. At Sfânta Ana, a volcanic crater lake with no outflow, water levels began to rise only after 7.4 ka (Magyari et al., 2009).

Several Holocene speleothem records are available from the Romanian Carpathians (Onac et al., 2002; Tămaş et al., 2005; Constantin et al., 2007). Trends towards higher values seen in these time series throughout the Holocene were interpreted as reflecting rising temperatures. McDermott et al. (2011) expanded the interpretation of individual European speleothem records and suggested a decreasing rainout gradient across the Holocene along a longitudinal transect. However, a more specific distinction between hydrology and temperature-driven changes is not easily achieved because interpreting stable oxygen isotope records from speleothems in terms of palaeoclimate is not generally straightforward (McDermott, 2004; Lachniet, 2009; Tremaine et al., 2011). For instance, the effects of temperature and climate–hydrology changes may cancel each other out, for example if there is a change in rainfall seasonality. Changes in seasonality of both rainfall and calcite precipitation are difficult to detect (Baker et al., 2011). Furthermore, moisture sources and transport trajectories, which generally affect the stable isotopic composition of meteoric water in Europe (Rozanski et al., 1982), may respond to regional-scale climate changes in contrast to local ones. Consequently, specific temperature or hydrological information is rarely directly quantifiable from speleothem stable isotope records. An example is the muted or even absent signal around the 8.2 ka cold event in speleothem δ^{18}O records throughout Romania (Tămaş et al., 2005; Constantin et al., 2007), despite this event being clearly identifiable in peat bog pollen records (Feurdean et al., 2007), in Balkan lake records (Pross et al., 2009; Panagiotopoulos et al., 2013), as well as in the Aegean Sea (Marino et al., 2009). This ambiguity of speleothem δ^{18}O records with respect to climatic events and transitions raises the question of how more specific information on the nature of climate change can be extracted from this proxy.

In this study we present a new speleothem isotopic record from Ascunsă Cave located on the eastern slopes of the Carpathian Mountains in Southern Romania (Fig. 1), in an area under periodical Mediterranean hydroclimate influences (Bojariu and Paliu, 2001; Apostol, 2008). We combine information from regionally averaged pollen-based temperature reconstructions from Europe across the Holocene (Davis et al., 2003) with the new oxygen isotope data from Ascunsă Cave, alongside a detailed comparison with published speleothem records from Romania (Onac et al., 2002; Tămaş et al., 2005; Constantin et al., 2007) and the Mediterranean (McDermott et al., 1999; Bar-Matthews et al., 2003; Drysdale et al., 2006; Vollweiler et al., 2006; Verheyden et al., 2008; Fleitmann et al., 2009). We also attempt to constrain the regional-scale hydrologic information inherent by speleothem δ^{18}O change across the Holocene, focusing on Mediterranean climate trends observable after 6 ka
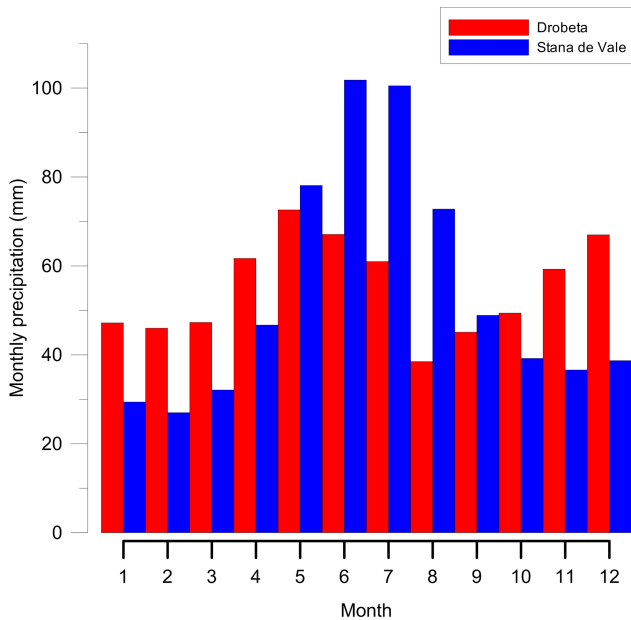
Figure 2. Average monthly precipitation quantities at stations Drobeta and Stâna de Vale (data from Dragotă and Baciu, 2008).

(Mayewski et al., 2004; Roberts et al., 2008, 2011; McDermott et al., 2011). Finally, local pollen data sets (Feurdean et al., 2008; Bordon et al., 2009) are used to constrain selected rapid climate shifts associated with the 8.2 ka and the 3.2 ka events.

2 Materials and methods

2.1 Cave setting and stalagmite characteristics

Ascunsă Cave is located on the eastern slopes of Mehedinţi Mountains, Southern Carpathians (45.0° N, 22.6° E, 1050 m alt.) in southwestern Romania (Fig. 1). It is a 400 m long and over 200 m deep contact cave developed by river erosion of Turonian–Senonian wildflysch (mélange) below an Upper Jurassic–Aptian limestone cover (Codarcea et al., 1964).

The cave is well decorated with speleothems and throughout its course there is a chaotic mixture of collapsed blocks and speleothem fragments reflecting the undermining of the wildflysch walls by fluvial erosion or their failure to support massive flowstone formations.

The analysed stalagmite (POM2) is 77.4 cm long and composed of well-laminated and densely compacted white calcite (Figs. 3 and 4). Topographic survey at the cave site revealed that limestone thickness above the stalagmite sampling site is ∼ 100 m.
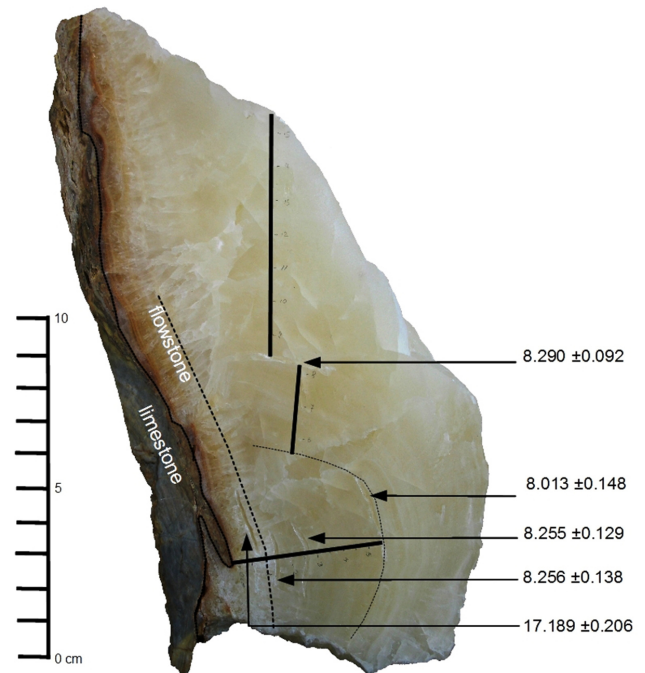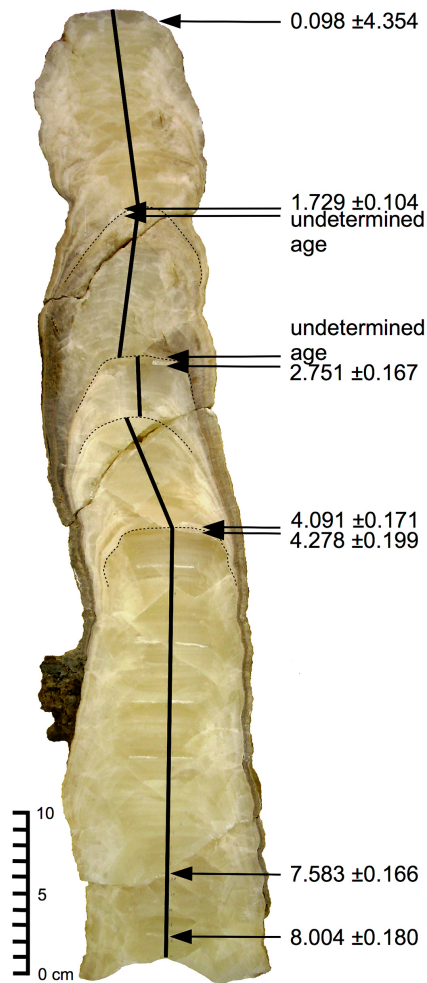

Figure 3. Base of stalagmite POM2 (ages are given in ka).

2.2 Present day climatology of the study area and cave monitoring

The regional climate of the Romanian Carpathians is temperate–continental, characterised by a predominantly Atlantic origin of air masses (Baltă and Geicu, 2008). It is also influenced (in the southwestern part) by Mediterranean cyclonic activity that is responsible for milder temperatures and increased winter rainfall in the area of the study site compared to northern or eastern Carpathians (Bojariu and Paliu, 2001; Apostol, 2008). Most of the cyclones affecting the study area originate in the central Mediterranean (around the Gulf of Genoa), but cyclones from the Aegean Sea also reach this region periodically (Apostol, 2008). Seasonal variability is observed in the formation of these cyclones, as shifts of the polar jet stream in winter affect Mediterranean cyclogenesis (Trigo et al., 2002).

Figure 2 illustrates the seasonal differences in precipitation recorded between 1961 and 2000 at two meteorological stations relevant for this study, Drobeta (SW Romania) and Stâna de Vale (W Romania) (data from Dragotă and Baciu, 2008). There is a clear difference in rainfall seasonality between the two regions, with Stâna de Vale having one rainfall peak in the summer, whereas at Drobeta two main rainfall periods are peaking in spring and early winter (Fig. 2).

Ascunsă Cave was monitored between July 2012 and November 2013 for atmospheric physical parameters and drip water isotopic composition. Temperature (T), relative humidity (RH) and CO_2 concentrations were measured at three sampling locations (POM A, POM2, and POM B)
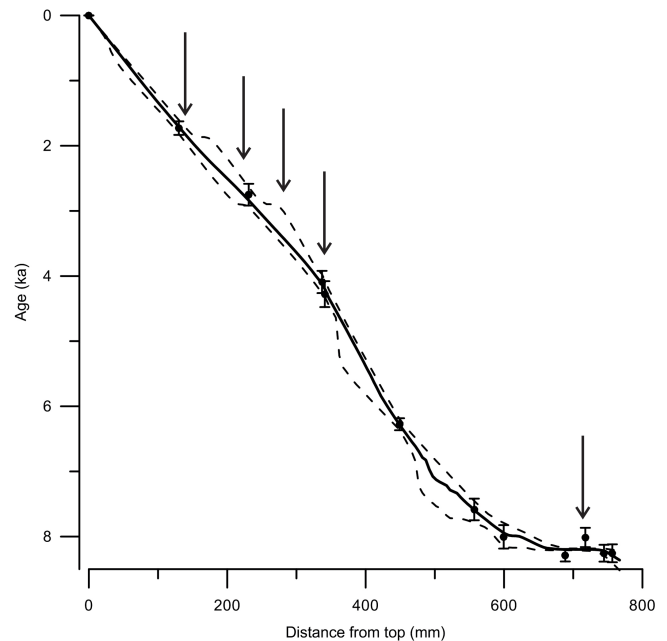
Figure 4. Upper part of stalagmite POM2 (ages are given in ka).

Figure 5. The growth model (solid line) of stalagmite POM2 with 95 % confidence intervals (dashed lines). Arrows indicate growth axis changes.

within Ascunsă Cave, using two Vaisala probes, GMP222 for CO_2 and HMP75 for T and RH. Drip water collected from stalactite tips at the sampling sites was analysed for $\delta^{18}O$ and δD on a Picarro L2130-i Cavity Ring-Down Spectroscope at Babeş-Bolyai University (Cluj-Napoca, Romania) following the method described by Brand et al. (2009). The analytical precision is better than ± 0.03 ‰ for $\delta^{18}O$ and ± 0.07 ‰ for δD. For data normalisation, two laboratory reference waters (VEEN and HTAMP) that were calibrated directly against VSMOW were measured repeatedly in each run. Results are expressed in ‰ on the VSMOW scale.

2.3 U-series dating and stable isotope analysis of speleothem samples

For U–Th dating, calcite samples were analysed on a THERMO Neptune MC-ICP-MS following procedures outlined in Hoffmann et al. (2007) and Hoffmann (2008). In total, 14 U–Th samples were measured, covering the entire length of the stalagmite. Three pairs of samples were drilled

immediately underneath and above visible changes in growth axis at 43.4, 54.4 and 63.9 cm.

A total of 150 stable isotope samples were hand drilled at 5 mm resolution using a 0.5 mm drill bit. All samples were analysed at the University of Oxford on a Thermo Delta V Advantage mass spectrometer equipped with a Kiel IV Carbonate Device. Results are reported relative to the Vienna Pee Dee Belemnite (VPDB) standard, and external precision on replicate samples (NBS 18, NBS 19, and a local carbonate standard) run daily on this system was 0.06 ‰ for $\delta^{18}O$ and 0.03 ‰ for $\delta^{13}C$.

3 Results and discussion

3.1 U-series dating results and growth model

The U–Th ages suggest that the stalagmite started growing around 17.2 ka, but most of the growth occurred between 8.2 ka and the present. The age model for the Holocene part of the stalagmite (Fig. 5) is based on 11 U–Th ages with typical dating uncertainties ranging between 1 and 6 % ($2\,\sigma$) (Table 1). The stalagmite was active at the time of sampling, thus the age at the top (77.4 cm) is assumed to be 0 (relative to 2009, the year of sampling) and is used as an additional tie point in the growth model calculation. The ^{238}U concentration varies between 18 and 50 ng g^{-1}, and ^{232}Th concentration ranges between 0.1 and 12.2 ng g^{-1}. Dating uncertainties are therefore mainly resulting from small U concentration and a significant correction

Table 1. Results of the U–Th measurements of POM2 samples.

Sample ID	Distance from bottom	^{238}U	^{232}Th	^{230}Th	[^{230}Th/^{232}Th]	(^{232}Th/^{238}U)	(^{230}Th/^{238}U)	(^{234}U/^{238}U)	Uncorrected age	Corrected age	Corrected (^{234}U/^{238}U)$_{initial}$
	(cm)	(ng g^{-1})	(ng g^{-1})	(ng g^{-1})	activity ratio	activity ratio	activity ratio	activity ratio	(ka)	(ka)	activity ratio
POM 09-2/top	76.35	18.26 ± 0.11	12.155 ± 0.074	3.951E-05 ± 3.44E-06	0.61 ± 0.05	2.178E-01 ± 6.002E-04	1.322E-01 ± 1.051E-02	1.791E+00 ± 7.699E-03	8.330 ± 0.685	0.098 ± 4.354	1.9098 ± 0.070
POM 09-2/I	63.35	18.94 ± 0.09	0.330 ± 0.003	1.122E-05 ± 3.29E-07	6.34 ± 0.18	5.706E-03 ± 4.247E-05	3.620E-02 ± 1.021E-03	2.087E+00 ± 6.154E-03	1.908 ± 0.055	1.729 ± 0.104	2.0960 ± 0.006
POM 09-2/III	62.85	18.99 ± 0.10	8.833 ± 0.044	2.264E-05 ± 6.54E-07	0.48 ± 0.01	1.522E-01 ± 4.452E-04	7.281E-02 ± 1.867E-03	1.848E+00 ± 6.245E-03	4.377 ± 0.115	–	–
POM 09-2/VI	53.75	19.11 ± 0.10	10.289 ± 0.054	2.100E-05 ± 6.81E-07	0.38 ± 0.01	1.761E-01 ± 4.941E-04	6.713E-02 ± 2.375E-03	1.969E+00 ± 7.584E-03	3.779 ± 0.136	–	–
POM 09-2/II	53.25	21.07 ± 0.11	0.605 ± 0.005	1.945E-05 ± 4.97E-07	6.00 ± 0.15	9.393E-03 ± 7.452E-05	5.639E-02 ± 1.441E-03	2.041E+00 ± 9.131E-03	3.052 ± 0.080	2.751 ± 0.167	2.0555 ± 0.010
POM 09-2/V	42.65	19.12 ± 0.09	0.588 ± 0.005	2.595E-05 ± 4.27E-07	8.24 ± 0.14	1.007E-02 ± 8.008E-05	8.293E-02 ± 1.451E-03	2.091E+00 ± 6.276E-03	4.405 ± 0.080	4.091 ± 0.171	2.1102 ± 0.007
POM 09-2/IV	42.25	19.62 ± 0.08	0.705 ± 0.006	2.775E-05 ± 5.81E-07	7.35 ± 0.15	1.175E-02 ± 9.093E-05	8.640E-02 ± 1.596E-03	2.066E+00 ± 8.421E-03	4.649 ± 0.090	4.278 ± 0.199	2.0868 ± 0.009
POM 09-2/VIII	32.3	42.96 ± 0.15	0.378 ± 0.004	7.403E-05 ± 9.71E-07	36.55 ± 0.52	2.794E-03 ± 2.624E-05	1.053E-01 ± 1.252E-03	1.849E+00 ± 4.267E-03	6.373 ± 0.079	6.275 ± 0.092	1.8658 ± 0.0044
POM 09-2/base	20.65	29.44 ± 0.17	0.597 ± 0.006	6.075E-05 ± 9.79E-07	19.00 ± 0.31	6.636E-03 ± 6.077E-05	1.261E-01 ± 1.884E-03	1.815E+00 ± 5.368E-03	7.820 ± 0.123	7.583 ± 0.166	1.8361 ± 0.006
POM 09-2/B	16.4	39.99 ± 0.20	0.245 ± 0.003	8.434E-05 ± 1.89E-06	64.38 ± 1.29	2.001E-03 ± 1.936E-05	1.289E-01 ± 2.710E-03	1.798E+00 ± 4.065E-03	8.077 ± 0.176	8.004 ± 0.180	1.8176 ± 0.004
POM 09-2/C	7.5	49.04 ± 0.25	0.228 ± 0.002	1.044E-04 ± 1.12E-06	85.37 ± 0.90	1.524E-03 ± 1.058E-05	1.301E-01 ± 1.302E-03	1.759E+00 ± 3.910E-03	8.346 ± 0.089	8.290 ± 0.092	1.7776 ± 0.004
POM 09-2/A	4.6	24.02 ± 0.11	0.097 ± 0.001	4.984E-05 ± 8.74E-07	95.85 ± 1.71	1.323E-03 ± 1.147E-05	1.268E-01 ± 2.200E-03	1.773E+00 ± 4.037E-03	8.062 ± 0.146	8.013 ± 0.148	1.7911 ± 0.004
POM 09-2/XXII	2.7	28.59 ± 0.09	0.140 ± 0.002	6.261E-05 ± 9.18E-07	83.63 ± 1.37	1.552E-03 ± 1.992E-05	1.338E-01 ± 1.928E-03	1.816E+00 ± 5.327E-03	8.311 ± 0.126	8.255 ± 0.129	1.8361 ± 0.0054
POM 09-2/XXIII	1.45	31.08 ± 0.10	0.190 ± 0.002	7.192E-05 ± 1.06E-06	71.51 ± 1.08	1.918E-03 ± 2.125E-05	1.414E-01 ± 2.172E-03	1.916E+00 ± 5.269E-03	8.321 ± 0.134	8.256 ± 0.138	1.9387 ± 0.0054
POM 09-2/D	0	20.72 ± 0.12	0.406 ± 0.004	1.060E-04 ± 1.17E-06	48.78 ± 0.53	6.407E-03 ± 4.260E-05	3.126E-01 ± 3.102E-03	2.097E+00 ± 4.978E-03	17.384 ± 0.190	17.189 ± 0.206	2.1563 ± 0.006

for initial Th, combined with the young age of the stalagmite which yields low ^{230}Th / ^{232}Th activity ratios (< 10) for six of the age determinations. Two samples (POM 09-2 / III and POM 09-2 / VI) were entirely dominated by detrital Th, with ^{230}Th / ^{232}Th activity ratios < 0.5 and have not yielded resolvable U–Th ages.

We measured U and Th isotopes on a sample from the top of the actively forming stalagmite in order to assess a reliable correction factor. The results show a ^{238}U concentration of 18.3 ± 0.1 ng g^{-1} and a ^{232}Th concentration of 12.2 ± 0.1 ng g^{-1}. The measured ^{230}Th in the top sample is assumed to be entirely of detrital origin and the apparent age of 8.3 ka a result of initial thorium contamination. The ^{230}Th/^{232}Th activity ratio of this sample is 0.6 ± 0.05, which indicates detrital activity ratios for ^{230}Th/^{232}Th, ^{234}U/^{232}Th and ^{238}U/^{232}Th of 0.6 ± 0.05, if we assume the detritus to be in secular equilibrium. We note that this factor is well within the range of the bulk earth value of 0.8 ± 0.4 (Wedepohl, 1995). We therefore use the value of 0.6 with a conservative uncertainty of 50 % to correct for initial Th.

The growth model of stalagmite POM2 (Fig. 5) was generated using the StalAge algorithm of Scholz and Hoffmann (2011).

3.2 Cave monitoring results

Monitoring data show a stable average temperature of $8.2 \pm 0.6\,°C$ at the stalagmite site. Relative humidity is also stable around $94 \pm 2.5\,\%$ during the year, especially at sampling sites POM2 (where stalagmite POM2 was sampled) and POM B situated deeper inside the cave (Table 2).

Isotope measurements of drip waters at POM2 site show rather consistent values for both δ^{18}O (-10.57 ± 0.04 ‰) and δD (-70.58 ± 0.20 ‰), during the autumn–winter months. This may indicate an efficient mixing of waters in the aquifer, without capturing any individual rain events.

Analysis of calcite farmed on glass plates also revealed relatively constant values with mean δ^{13}C of -10.30 ± 0.8 ‰ and δ^{18}O of -7.91 ± 0.2 ‰ for both POM2 and an adjacent stalagmite, POM X (Table 3).

We constructed a local drip water line for Ascunsă Cave (Fig. 6) using δ^{18}O and δD values of drip waters from all three sampling sites. Compared to the global (GMWL) and Mediterranean (MMWL) meteoric water lines, the Ascunsă groundwater line (AGWL) is defined as $\delta D = 6.9 \times \delta^{18}O + 2$ and plots above the GMWL. This suggests a mixture of Atlantic and Mediterranean moisture. The slope of the local water line is slightly lower than that of the GMWL and MMWL, respectively. This may be an indication of slight enrichment due to evaporation from the soil above the cave.

Table 2. Spot measurements of physical climate parameters in Ascunsă Cave, including water stable isotopes.

Date	Air T (°C)	RH (%)	CO_2 (ppm)	$\delta^{18}O$ (‰, SMOW)	δD (‰, SMOW)
POM A					
13 July 2012	7.5	93.7	1300	N/A	N/A
17 October 2012	N/A	N/A	N/A	−10.39	−69.63
30 November 2012	8.2	92.0	1520	N/A	N/A
4 January 2013	7.8	89.4	1050	−10.36	−68.91
28 February 2013	7.2	N/A	760	−10.39	−68.87
20 April 2013	7.5	96.8	870	−10.83	−72.43
26 May 2013	8.4	92.3	1070	N/A	N/A
21 September 2013	8.6	90.25	1060	N/A	N/A
2 November 2013	8.7	89.3	1710	N/A	N/A
POM2					
13 Jul 2012	8.2	94.0	1280	N/A	N/A
17 October 2012	N/A	N/A	N/A	−10.571	−70.74
30 November 2012	8.2	94.2	1740	−10,582	−70.54
4 January 2013	8.1	94.1	1770	−10.517	−70.35
28 February 2013	7.6	N/A	1400	−10.596	−70.67
20 April 2013	7.9	96.8	960	−10.760	−71.72
26 May 2013	8.8	92.2	1150	N/A	N/A
21 September 2013	8.3	94.68	1360	N/A	N/A
2 November 2013	8.6	91.25	1820	N/A	N/A
POM B					
13 Jul 2012	8.4	93.1	1300	N/A	N/A
17 October 2012	N/A	N/A	N/A	−10.68	−71.46
30 November 2012	8.5	93.0	1880	−10.39	−70.01
4 January 2013	8.6	92.0	1660	−10.46	−69.77
28 February 2013	7.8	N/A	1360	−10.37	−69.15
20 April 2013	8.6	94.3	1110	−10.94	−73.24
26 May 2013	9.6	88.6	1270	N/A	N/A
21 September 2013	8.5	93.95	1550	N/A	N/A
2 Nov 2013	8.6	93.3	2010	N/A	N/A

To test the existence of equilibrium fractionation conditions at the POM2 site, we used drip water $\delta^{18}O$ values to calculate a theoretical $\delta^{18}O$ value of the farmed calcite, using the equation given by Tremaine et al. (2011):

$$1000 \ln \alpha = 16.1(\pm 0.65) \times 10^3 T^{-1} - 24.6(\pm 2.2).$$

The resulting value of -8.5 ± 0.1 ‰ is slightly below the average of -7.9 ‰ measured on calcite farmed at POM2 and POM X sites. The 0.6 ‰ offset from generally predicted values could indicate some kinetic fractionation. However, the average drip water value derived from point-sampling in time may not exactly represent the annual amount-weighted average rainfall and its isotopic composition. As such, calcite precipitation may still be considered to have taken place close to equilibrium during the monitored period. The offset is somewhat larger when the calibration of Kim and O'Neill (1997) or Day and Henderson (2011) are used (-9.2 ‰ and -9.6 ‰, respectively). In this study, we base our calculations on the

empirical equation of Tremaine et al. (2011), which appears to better characterise conditions in Ascunsă Cave.

3.3 Speleothem records

3.3.1 The $\delta^{18}O$ record in Romanian speleothems

The most prominent feature of the $\delta^{18}O$ isotopic profile of stalagmite POM2 (Fig. 7) is a trend towards higher values during the middle Holocene. This trend shows some similarity to the stacked eastern Mediterranean lacustrine $\delta^{18}O$ record (Roberts et al., 2011). In order to place the Ascunsă Cave $\delta^{18}O$ trend across the mid-Holocene into a regional context, we compare our record with $\delta^{18}O$ profiles of stalagmites from Poleva Cave (Constantin et al., 2007), Urşilor Cave (Onac et al., 2002) and V11 Cave (Tămaş et al., 2005). We also added $\delta^{18}O$ values calculated by McDermott et al. (2011) as representative of European caves at 22° E
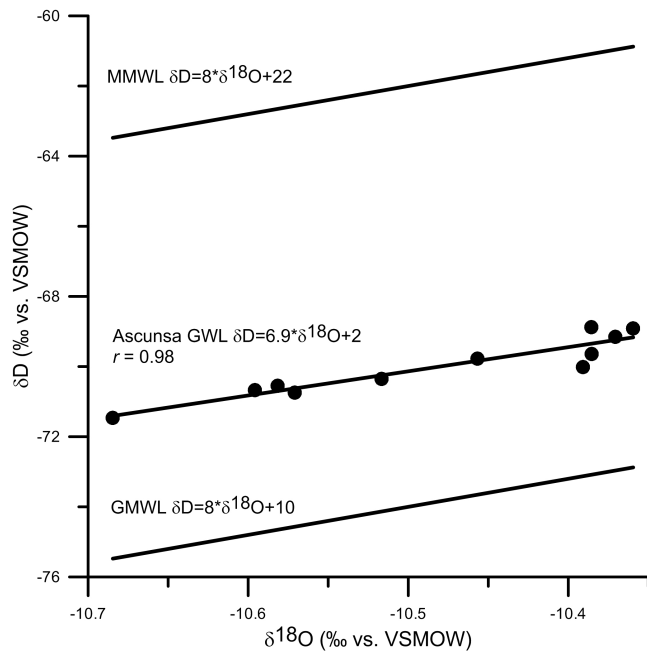
Figure 6. Comparison between global meteoric water lines (GMWL; Craig, 1961) and Mediterranean meteoric water lines (MMWL; Gat and Carmi, 1970), as well as Ascunsă Cave groundwater line.

Table 3. Stable isotope values of farmed calcite in Ascunsă Cave.

Sample	$\delta^{13}C$	$\delta^{18}O$
POM A Sep 2010–Jan 2011	−10.657	−8.264
POM A Jan 2011–Jul 2012	−9.455	−7.510
POM A Jul 2012–Oct 2012	−9.485	−7.826
POM2 Jan 2011–Jul 2012	−10.403	−7.550
POM2 Jul 2012–Oct 2012	−10.369	−7.844
POM2 Dec 2012– Jan 2013	−10.434	−7.964
POM2 Jan 2013–Apr 2013	−11.129	−8. 097
POM X Sep 2010–Jan 2011	−9.801	−8.312
POM X Jan 2011–Jul 2012	−10.427	−7.877
POM X Jul 2012–Oct 2012	−9.594	−7.780
POM X Oct 2012–Dec 2012	−10.234	−7.912
POM X Dec 2012–Feb 2013	−10.009	−7.869
POM X Feb 2013–Apr 2013	−10.360	−7.915

longitude at low altitudes (Fig. 8a). The general trends of measured values agree to a variable degree with modelled Rayleigh distillation of Atlantic air masses at low altitude (McDermott et al., 2011). A somewhat more negative measured $\delta^{18}O$ overall at Ascunsă Cave (Fig. 8b) could reflect the higher altitude of the cave and higher rainout on route leading to increasingly lower $\delta^{18}O$ in the moisture arriving at the cave site, but the observed trend may not be explained completely by this model. Poleva Cave shows slightly higher calcite $\delta^{18}O$ values after 4 ka (−7.6 ‰) in comparison to > 6 ka (−8.3 ‰) and Constantin et al. (2007) interpret this increase as a general warming trend. At Urșilor Cave (NW Romania), late Holocene $\delta^{18}O$ values are slightly higher (by 0.2 ‰) than during the middle Holocene and Onac et al. (2002) suggests that an apparent lack of variability at this site reflects relatively stable climate conditions.

Well-known rapid climate change events (Mayewski et al., 2004) such as the 8.2 ka event are not always clearly expressed in Romanian speleothem $\delta^{18}O$ records (Onac et al., 2002; Tămaș et al., 2005; Constantin et al., 2007). This absence in the speleothem $\delta^{18}O$ record is in contrast to reports from the marine records from the eastern Mediterranean (Rohling et al., 2002), and lacustrine records from the wider Balkan region (Feurdean et al., 2008, Pross et al., 2009). An exception is a common negative excursion occurring at ∼ 3.2 ka that is recorded in the $\delta^{18}O$ time series of Ascunsă and Poleva caves in the Southern Carpathians. This century-long cold event has been identified in marine records

from the eastern Mediterranean (Rohling et al., 2002) and in lacustrine records from the Balkan region (Feurdean et al., 2008).

3.3.2 Constraining regional temperature change in the speleothem $\delta^{18}O$ record with independent temperature reconstructions

Stable oxygen isotopes in individual speleothems are potentially influenced by local effects, such as cave hydrology and cave ventilation, which may obscure the regional climate signal (Tremaine et al., 2011; Riechelmann et al., 2013). Here, we employ coeval data recorded in more than one cave to account for such potential biases. We specifically address the three features reported above: (1) the general mid-Holocene trend by comparing the isotopic difference between 2000 years averaged time intervals between the early and late Holocene, from 8–6 ka and 4–2 ka, respectively (Fig. 8a); (2) the absence of an unambiguous 8.2 ka event in isotopic speleothem records from Romania, and (3) the nature of a clear isotope excursion ∼ 3.2 ka in two Southern Carpathian speleothems.

The principal controls of oxygen isotope fractionation during speleothem calcite precipitation are temperature in the cave and isotopic composition of drip water (e.g. Day and Henderson, 2011; Tremaine et al., 2011). Both aspects directly respond to changes of annual average air temperature above the cave. In addition, drip water $\delta^{18}O$ may also record variations in hydrologic climate characteristics, such as rainfall seasonality, evaporation, moisture sources and rainout efficiency along the path (McDermott, 2004; Fairchild et al., 2006; Lachniet, 2009). The two principal contributors to change – temperature and climate hydrology – may be separated as follows: assuming that (1) calcite precipitation temperature in the cave reflects the annual average surface air temperature and oscillates very little year-round (see also

‰ vs. VPDB
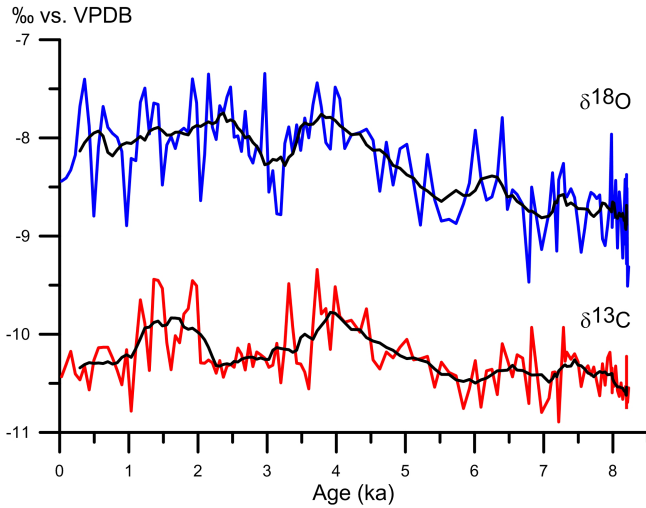
Figure 7. $\delta^{18}O$ and $\delta^{13}C$ profiles of stalagmite POM2 with nine-point smoothed values (black).

Table 4. Regional pollen data sets (after Davis et al., 2003) and from Steregoiu (Feurdean et al., 2008) used for the calculation of the temperature effect on speleothem isotopic values between 6 and 4 ka. Steregoiu data were converted to temperature anomalies with respect to the latest 100 years.

Pollen region	Average TA 8–6 ka	Average TA 4–2 ka	ΔTA 6–4 ka
TANN CW Europe	−0.26	−0.08	0.18
TANN SE Europe	−0.51	0.04	0.56
TANN CE Europe	1.29	1.02	−0.27
TANN SW Europe	−2.03	−0.82	1.21
TANN Steregoiu	0.00	0.60	0.59
MTWA CW Europe	0.32	0.18	−0.14
MTWA SE Europe	−0.88	−0.41	0.47
MTWA CE Europe	0.36	0.10	−0.26
MTWA SW Europe	−1.72	−0.67	1.05
MTWA Steregoiu	0.45	1.35	0.91
MTCO CW Europe	−0.49	0.37	0.87
MTCO SE Europe	0.20	0.31	0.11
MTCO CE Europe	0.29	0.12	−0.16
MTCO SW Europe	−1.51	−0.38	1.13
MTCO Steregoiu	−0.90	−0.58	0.32

Table 2) and (2) the coldest and warmest months define the range of temperature-controlled oxygen isotope fractionation during condensation of rain, one may calculate an expected range for relative changes in speleothem $\delta^{18}O$ based entirely on temperature variation. To do this, we employ pollen-based temperature reconstructions of the annual average surface air temperature (TANN – Temperature ANNual), surface air temperature of the coldest month (MTCO – Mean Temperature of the COldest month), and surface air temperature of the warmest month (MTWA – Mean Temperature of the WArmest month) for two zonal sectors from central Europe and the Mediterranean, respectively (Davis et al., 2003), to derive a pollen temperature-constrained range of expected $\delta^{18}O$ change ($\Delta\delta^{18}O_{c\_ptc}$).

In this calculation, we use the empirical equation of Tremaine et al. (2011) for temperature-dependent oxygen isotope fractionation during calcite precipitation:

$$1000\ln\alpha = 16.1(10^3 T^{-1}) - 24.6. \tag{1}$$

For the $\delta^{18}O$–temperature relationship in rainwater we use the empirical global mid-latitude relationship suggested by Rozanski et al. (1993):

$$\delta^{18}O_{w}/\Delta T = 0.58‰\,°C^{-1}. \tag{2}$$

For calcite precipitation, $\Delta\delta^{18}O_c / \Delta T$ is $\sim -0.18\,‰\,°C^{-1}$ (Tremaine et al., 2011). Therefore, the combined effect of temperature change in speleothem calcite ($\Delta\delta^{18}O_{c\_spel}$) is dominated by rainfall temperature change and resulting changes in drip water $\delta^{18}O_{w}(\Delta\delta^{18}O_c \approx -1/3\,\Delta\delta^{18}O_{w})$. Sources of error in this approach are discussed along with the details of calculation in the Appendix. We compare the calculated temperature-constrained range of relative $\delta^{18}O$ variation – the range of $\Delta\delta^{18}O_{c\_ptc}$ – with $\Delta\delta^{18}O_{c\_spel}$ observed in

several Romanian speleothem records in order to identify the likelihood of additional changes in other climate–hydrology related parameters (e.g. rainfall seasonality, evaporation from the soil, or variable moisture sources and pathways).

If only temperature variability contributed to the observed difference between two time intervals of interest, $\Delta\delta^{18}O_{c\_spel}$ will plot inside the expected pollen temperature-constrained range of values (range of $\Delta\delta^{18}O_{c\_ptc}$) calculated from the pollen input data TANN, MTCO and MTWA. If rainfall seasonality changes along with temperature, $\Delta\delta^{18}O_{c\_spel}$ may still fall inside the range of $\Delta\delta^{18}O_{c\_ptc}$ – if changes in rainfall seasonality are relatively small – or outside, depending on the combination of changing temperature seasonality and rainfall seasonality. Example calculations can be easily performed (not shown) and they demonstrate that, for example, in the case of warming an additional change towards a more pronounced rainfall seasonality with a higher proportion of summer rain would result in $\Delta\delta^{18}O_{c\_spel}$ falling above the range of $\Delta\delta^{18}O_{c\_ptc}$. If rainfall seasonality changed towards more winter rain under the same warming scenario, $\Delta\delta^{18}O_{c\_spel}$ would fall below the range of $\Delta\delta^{18}O_{c\_spel}$ from the range of $\Delta\delta^{18}O_{c\_ptc}$. A cooling scenario instead of a warming one would produce the same relationship between $\Delta\delta^{18}O_{c\_spel}$ and $\Delta\delta^{18}O_{c\_ptc}$, but the sign of both $\Delta\delta^{18}O$ would be negative. A significant change in rainfall seasonality in addition to a change in any other climate–hydrology parameter – such as evaporation from the soil or moisture source and pathways, for example the relative contribution of Atlantic and Mediterranean moisture – would
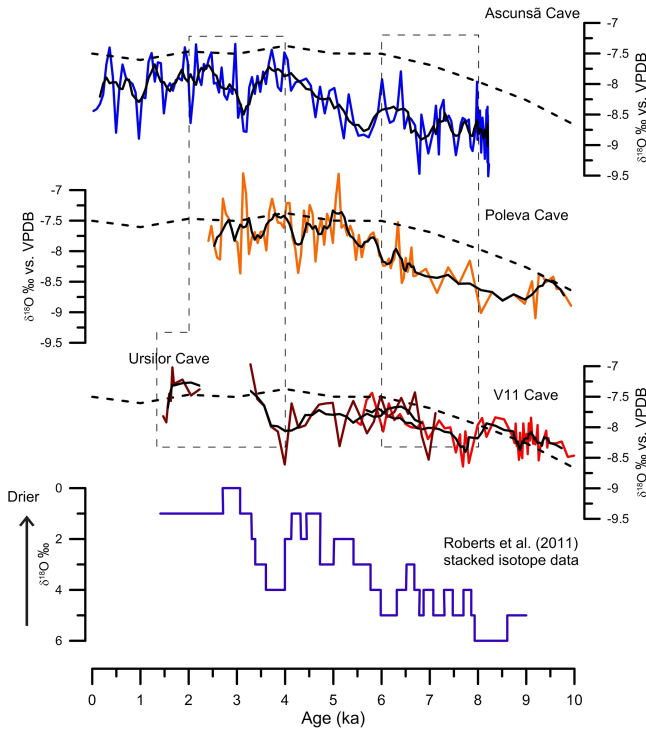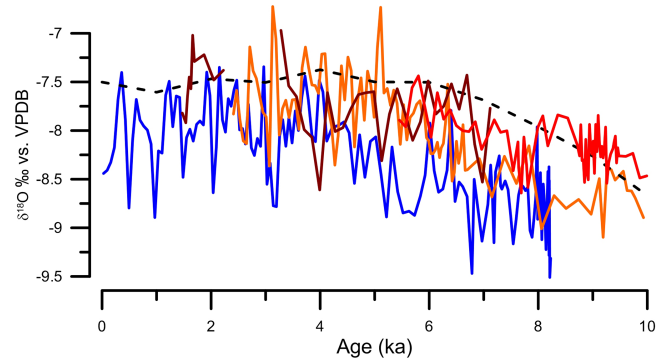
Figure 8a. Comparison between δ^{18}O records from Ascunsă, Poleva, Urşilor and V11 caves. Isotopic values from a Rayleigh distillation model (McDermott et al., 2011) for low-altitude caves at 22° E longitude are represented as dashed line. Stacked ISOMED lacustrine δ^{18}O for Mediterranean lakes after Roberts et al. (2008). Dashed-line boxes represent the time windows (4–2 and 8–6 ka) used in the calculation (see text).

Figure 8b. Stack of δ^{18}O records from Ascunsă, Poleva, Urşilor and V11 caves. Isotopic values from a Rayleigh distillation model (McDermott et al., 2011) for low-altitude caves at 22° E longitude are represented as dashed line.

further add to the distance of $\Delta\delta^{18}$O$_{c\_spel}$ from the range of $\Delta\delta^{18}$O$_{c\_ptc}$.

3.3.3 Temperature and hydrology-related changes in speleothem δ^{18}O records from Romania and the Mediterranean basin

We analyse the broad δ^{18}O change across the time interval 6–4 ka as outlined above for the Romanian stalagmites and also for a selection of southern European records (Fig. 9). The pollen-based temperature reconstruction by Davis et al. (2003) divides Europe into six main regions: northwestern (NW), northeastern (NE), central-western (CW), central-eastern (CE), southwestern (SW) and southeastern (SE). The boundary between central and southern zones is 45° N, the boundary between western and eastern zones is 15° E. This places the Alps and much of northern Italy inside the CW zone and divides Romania between the CE and SE zone along the Southern Carpathians. Across the last 8000 years the CW shows a slight winter warming, the CE zone shows only little change, the SW zone shows a 2 °C warming trend for both seasons, and the SE zone shows a 1 °C warming during summer (Davis et al., 2003). The specific regionally aver-
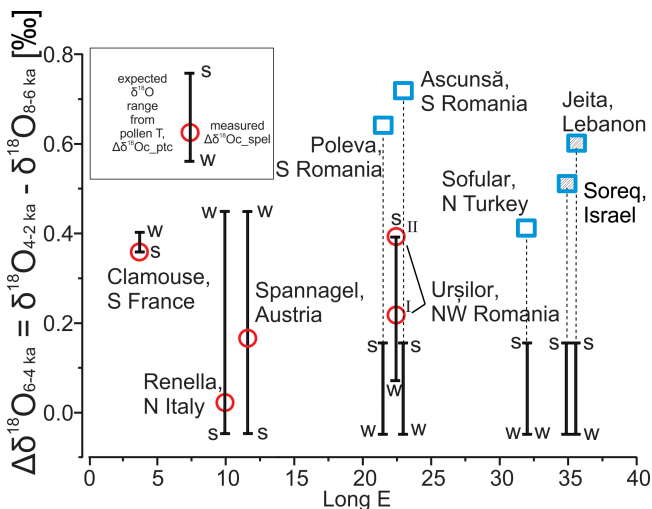
aged pollen data sets used to calculate isotopic variability in different cave records are summarised in Table 4 and calculation details are given in Table 5. Potential shortcomings of the chosen pollen zones are also discussed in the Appendix.

For Ascunsă Cave, which is inside the SE pollen zone of Davis et al. (2003), speleothem $\Delta\delta^{18}$O$_{6-4ka}$ is 0.69 ‰, whereas values expected from the pollen-based temperature reconstruction are between 0.16 ‰ (summer) and −0.05 ‰ (winter) (Fig. 9). This implies that across the middle Holocene transition speleothem δ^{18}O values at the cave site became higher than expected if only temperature change occurred. As δ^{18}O increases in the majority of observed speleothems from the eastern Mediterranean domain across the 6–4 ka interval beyond the temperature-controlled amount (Fig. 9), there must have been a common large-scale change of climate–hydrology. This may include a combination of change in rainfall seasonality with any other hydrological factor, such as local evaporation, a change in the proportion of Atlantic vs. Mediterranean moisture source (Rozanski et al., 1993), or a change in the isotopic composition of the two vapour sources.

To rule out local climate effects, we compare our speleothem record with other isotope records from Poleva (Constantin et al., 2006) and Urşilor (Onac et al., 2002) caves. Considering that the Davis et al. (2003) CE pollen zone is not well represented around 45° N latitude in Romania, we use the local temperature reconstruction derived from the pollen record of Steregoiu (Feurdean et al., 2008) for Urşilor Cave. Figure 9 shows that measured $\Delta\delta^{18}$O$_{6-4ka}$ at Poleva is similar to that at Ascunsă and falls well outside the pollen temperature-constrained range of change, whereas Urşilor falls within the constrained range close to the summer temperature value. Even if the Urşilor record is completed with nearby V-11 data to complement the 8–6 ka BP interval, $\Delta\delta^{18}$O$_{6-4ka}$ remains fully explained by $\Delta\delta^{18}$O$_{c\_ptc}$ (see Fig. 9). This is despite the fact that due to the higher altitude of V-11 cave, its δ^{18}O data are most likely skewed

Table 5. Speleothem isotope data and calculation results of temperature-constrained speleothem isotope values for the mid-Holocene transition.

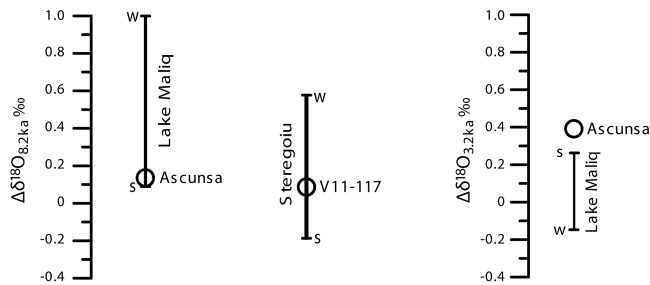| Site	$\delta^{-18}O_{c\_spel}$ 8–6 ka (VPDB)	$\delta^{-18}O_{c\_spel}$ 4–2 ka (VPDB)	$\Delta\delta^{18}O_{c\_spel}$ 6–4 ka (VPDB)	Cave T °C	TANN ΔTA 6–4 ka	$\Delta\delta^{18}O_{ct}$ 6–4 ka (VSMOW)	MTWA ΔTA 6–4 ka	MTCO ΔTA 6–4 ka	$\Delta\delta^{18}O_{w-summer}$ 6–4 ka (VSMOW)	$\Delta\delta^{18}O_{w-winter}$ 6–4 ka (VSMOW)	$\Delta\delta^{18}O_{c\_pct}$ 6–4 ka summer (VPDB)	$\Delta\delta^{18}O_{c\_pct}$ 6–4 ka winter (VPDB)
Ursilor	−7.80	−7.60	0.20	10.0	0.59	−0.12	0.91	0.32	0.53	0.19	0.39	0.07
Ursilor + V11	−8.00	−7.60	0.40	–	0.59	−0.12	0.91	0.32	0.53	0.19	0.39	0.07
Ascunsa	−8.65	−7.96	0.69	8.0	0.56	−0.11	0.47	0.11	0.27	0.07	0.16	−0.05
Poleva	−8.25	−7.62	0.63	10.0	0.56	−0.11	0.47	0.11	0.27	0.07	0.16	−0.04
Sofular	−8.53	−8.12	0.41	13.3	0.56	−0.11	0.47	0.11	0.27	0.07	0.16	−0.04
Soreq	−5.91	−5.40	0.51	18.0	0.56	−0.11	0.47	0.11	0.27	0.07	0.16	−0.04
Jeita	−5.40	−4.76	0.64	22.0	0.56	−0.10	0.47	0.11	0.27	0.07	0.17	−0.04
Renella	−3.96	−3.94	0.02	12.0	0.18	−0.04	−0.14	0.87	−0.08	0.50	−0.11	0.45
Clamouse	−4.92	−4.56	0.36	14.5	1.21	−0.24	1.05	1.13	0.61	0.65	0.36	0.40
Spannagel	−7.81	−7.64	0.17	1.9	0.18	−0.04	−0.14	0.87	−0.08	0.50	−0.11	0.45

Figure 9. Comparison of isotopic changes in stalagmites across different longitudes in Europe in the interval 6–4 ka, $\Delta\delta^{18}O_{c\_spel}$, with pollen temperature-constrained range of $\Delta\delta^{18}O_{c\_pct}$ (summer and winter) calculated by using data from Davis et al. (2003) and Feurdean et al. (2008). For Urșilor Cave, two options are shown: (I) $\Delta\delta^{18}O_{6-4\,ka}$ based on the Urșilor data alone, (II) $\Delta\delta^{18}O_{6-4\,ka}$ based on the combination of Urșilor and V-11 isotope data.

nagel Cave, Austria (Vollweiler et al., 2006), each in combination with the Davis et al. (2003) CW European temperature time series; and finally Sofular Cave, Turkey (Fleitmann et al., 2009), Soreq Cave, Israel (Bar-Matthews et al., 2003) and Jeita Cave, Lebanon (Verheyden et al., 2008), each in combination with the Davis et al. (2003) SE European temperature time series. The pollen reconstructions show rising temperatures throughout the year for the SW zone (Davis et al., 2003), whereas in the CW zone, increasing winter temperatures offset decreasing summer temperatures. The results are also shown in Fig. 9. It is apparent that isotope values from the western Mediterranean (Clamouse) and CW Europe south of the Alpine divide (Renella and Spannagel) show a change in $\delta^{18}O$ that is explained almost entirely by pollen-constrained temperature change. Only at the Renella site, could a small hydrologic influence be argued for, as the observed change is close to the summer end of the range (Fig. 9). This likely represents a shift towards the present-day rainfall domination by the winter season (Scholz et al., 2012). On the other hand, sites in Turkey (Sofular), Israel (Soreq), Lebanon (Jeita) and southern Romania (Poleva and Ascunsă) that are potentially influenced by the eastern Mediterranean plot well above the temperature-constrained change. Thus, it appears that across the middle Holocene transition, the entire eastern Mediterranean domain including the Southern Carpathians underwent a significant moisture-balance change in addition to some temperature change, whereas in the western Mediterranean and the southern Alps such change in climate–hydrology is not apparent.

In principle, three aspects may have contributed to the observed hydrologic change in the east: (1) a significant change in rainfall seasonality – in this case a higher proportion of summer rain, (2) a change in evaporation from the soil, (3) a change in proportion of moisture source or a different isotopic composition of the moisture sources. Higher $\delta^{18}O$ values in the speleothems after the change could be the result of more rain falling in the warm summer months (higher $\delta^{18}O_w$) during the late Holocene, but this scenario is unlikely because large-scale subsidence over the eastern Mediterranean region due to the Asian monsoon most likely strengthened (Staubwasser and Weiss, 2006). As a result, there is vir-

towards lower values in comparison to Urșilor (V-11 is at 1254 m, Urșilor is at 486 m). Altogether, the data suggest that the 6–4 ka transition at Ascunsă and Poleva in the Southern Carpathians marks a significant hydrologic change in southern Romania that is not obvious in the Apuseni Mountains of NW Romania. A similar gradient in the expression of Holocene climate change can also be found in other parts of Europe at these latitudes (see review in Magny et al., 2013).

To verify a suspected large-scale gradient in the nature of climate change across Southern Europe, we calculated similar pollen temperature-constrained $\delta^{18}O$ values for several cave records around the Mediterranean, across the same 6–4 ka transition. These records are: Grotte de Clamouse, France (McDermott et al., 1999), in combination with the Davis et al. (2003) SW European temperature time series; Buca della Renella, Italy (Drysdale et al., 2006) and Span-

Figure 10. Comparison of isotopic changes in speleothems ($\Delta\delta^{18}O_{c\_spel}$) for the 8.2 ka event (left) and 3.2 ka event (right) in stalagmites from Ascunsă and V11 caves with pollen temperature-constrained range of $\Delta\delta^{18}O_{c\_pct}$ (summer and winter) calculated by using data from Steregoiu peat bog (Feurdean et al., 2008 and Lake Maliq (Bordon et al., 2009).

tually no rainfall during summer in the Levant, and rainfall is significantly reduced over SE Europe. Precipitation is at a minimum in August in SW Romania (Fig. 2). Subsidence and accompanying low humidity over the eastern Mediterranean may, however, have increased evaporation from the soil, which would be in agreement with rising summer temperatures in SE Europe across the Holocene (Davis et al., 2003). Evaporation in the soil and epikarst drives drip water $\delta^{18}O$ towards more positive values, resulting in higher $\delta^{18}O$ in speleothem calcite (Bar-Matthews et al., 1996; Fairchild et al., 2006). A measurable effect of evaporation at Ascunsă may be implied from the slope of the local drip water line (see Sect. 3.2).

Alternatively, the proportion of summer rain could have been higher just because winter rainfall decreased. McDermott et al. (2011) suggested lower rainout efficiency during winter along a west–east transect across central Europe. However, higher winter temperatures were only observed in the western Mediterranean region (Davis et al., 2003, SW Europe quadrant). This would increase the temperature gradient between SW Romania and the source of cyclones in the Gulf of Genoa – which is inside the SW Europe quadrant – possibly increasing rainout efficiency in South Europe. An interesting analysis of synoptic-scale mid-tropospheric (500 mbar) pressure distribution of exceptionally wet winters in the Levant points to a possible physical mechanism causing the climate changes discussed above (Enzel et al. 2004). Such years coincide with a large-scale negative pressure anomaly centred over Asia Minor and the Middle East that encompasses all the eastern Mediterranean speleothem sites discussed above. Scenarios (1) enhanced summer evaporation and (2) reduced winter rainfall notably do not exclude each other.

The third factor that may have added to the observed increase in speleothem $\delta^{18}O$ is a change in the isotopic composition of the Mediterranean mixed layer. A steady increase in $\delta^{18}O$ by approximately 0.7‰ was derived from $\delta^{18}O$ in

tests of surface dwelling foraminifera and an independent sea surface temperature estimate for the Aegean Sea between 8 and 4 ka BP, which is uncorrelated with the abundance of cold water species (Marino et al., 2009). In the Adriatic Sea, an increase by 0.5‰ was recorded in $\delta^{18}O$ of foraminifera at the same time (Siani et al., 2010). As such, a combination of warmer summer temperatures, enhanced evaporation from the soil, and higher $\delta^{18}O$ of the eastern Mediterranean moisture source are currently the favoured explanation for the observed increase in $\delta^{18}O$ of speleothems across the mid-Holocene from the eastern Mediterranean domain.

3.3.4 The $\delta^{13}C$ record

Interpretation of speleothem $\delta^{13}C$ data (Fig. 7) is generally hampered by a host of local factors such as changes in soil CO_2 production and content, closed versus open system dissolution of carbonates in the soil/epikarst system, residence time and mixing of waters along the pathway to the drip point, or solution degassing (Hendy, 1971; Bar-Matthews et al., 1996; Fairchild et al., 2006).

Percolating water degassing could be greater during certain periods at POM2 sampling site, as the CO_2 content of the cave's atmosphere drops from ∼ 1800 ppm in November–December to ∼ 1000 ppm in April–May. This seasonal variation in the CO_2 content of cave air is likely the combined result of soil CO_2 productivity and cave ventilation (Spötl et al., 2005, Kowalczk and Froelich, 2010; Frisia et al., 2011; Tremaine et al., 2011; Riechelmann et al., 2013).

At the POM A site, which is the shallowest and closest to the entrance, the CO_2 concentration reaches a minimum value of 760 ppm, well above values of outside air (between 200 and 310 ppm). The two deeper sites, POM2 and POM B, show even less ventilation, with minimal values of 960 ppm. This indicates that cave ventilation is moderate (although continuous) at Ascunsă Cave.

Supposing that the cave ventilation regime remained unchanged during the middle Holocene, cave air CO_2 was probably controlled mostly by soil/vegetation dynamics. If so, higher speleothem $\delta^{13}C$ values are indicative of reduced CO_2 input from the soil and/or prior precipitated calcite (Fairchild et al., 2000). These two processes could be the result of drier conditions being established across the mid-Holocene and might have been responsible for producing the upward trend observed in $\delta^{13}C$ values between 6 and 4 ka BP.

3.3.5 The 8.2 ka and 3.2 ka events

The 8.2 ka climate change event (Alley et al., 1997; Rohling and Pälike, 2005) is one of the most prominent events of environmental change in the Holocene. Pollen assemblages from northern Romania (Feurdean et al., 2008), Macedonia (Bordon et al., 2009) and Greece (Pross et al., 2009), testate amoebae from northern Romania (Schnitchen et al., 2006), speleothem carbon stable isotopes from Israel (Bar-

Matthews et al., 2000) and marine faunal composition from the Aegean Sea (Rohling et al., 2002) document a decrease in winter temperature and precipitation, while summer conditions remained rather stable. Similar to other Romanian stalagmites (Tămaş et al., 2005; Constantin et al., 2007), the POM2 $\delta^{18}O$ and $\delta^{13}C$ records do not show significant variability across the 8.2 ka event. The only indication of changing environmental conditions is that the growth rate was six times higher during this event compared to the rest of the Holocene in the Ascunsă Cave.

Figure 10 shows a comparison of calculated $\Delta\delta^{18}O_{c\_ptc}$ measured $\Delta\delta^{18}O_{c\_spel}$ values for the 8.2 and 3.2 ka events. For the 8.2 ka event, $\Delta\delta^{18}O_{c\_ptc}$ is calculated as the difference between a 500-year interval succeeding the event (8.1–7.6 ka) and the event itself (8.3–8.1 ka). Here we used pollen-based temperature reconstructions as follows: for V11 Cave, those from the Steregoiu peat bog in northern Romania (Feurdean et al., 2008), and for Ascunsă Cave, the Lake Maliq in Macedonia (Bordon et al., 2009).

The shift in isotopic values after the 8.2 ka event at V-11 and Ascunsă Cave is well explained by the pollen-based temperature rise (Feurdean et al., 2008; Bordon et al., 2009). The pollen data suggest a significant warming in winter and very slight cooling in summer after the 8.2 ka cold event. Lake Maliq suggests a strong warming in winter and a lesser warming in summer after the event. $\Delta\delta^{18}O_{c\_spel}$ generally agrees with calculated $\Delta\delta^{18}O_{c\_pct}$ Nevertheless, as $\Delta\delta^{18}O_{c\_spel}$ from Ascunsă falls closer to the summer end of $\Delta\delta^{18}O_{c\_ptc}$, a climate-related hydrological influence on the speleothem data could be argued for. A $\Delta\delta^{18}O_{c\_spel}$ close to the low-$\delta^{18}O$ summer end of the calculated range of $\Delta\delta^{18}O_{c\_ptc}$ may be interpreted as a slight increase in the proportion of winter rain after the 8.2 ka event. Lower winter rainfall during the 8.2 ka event is in agreement with precipitation reconstruction from Lake Maliq and Steregoiu (Bordon et al., 2009; Feurdean et al., 2008), but the speleothem data would only support a small reduction of winter rain during the 8.2 ka event. However, a high speleothem precipitation rate during the 8.2 ka event may suggest a high infiltration rate and more rain. The apparent high infiltration rate of drip water could mean that instead of a reduction in winter rain, summer rainfall increased during the 8.2 ka event.

The 0.4 ‰ increase in $\delta^{18}O$ values in the Ascunsă record between the average of periods 3.2–2.9 ka and 2.9–2.5 ka defines the 3.2 ka event. Both Ascunsă and Poleva (Constantin et al., 2007) show a comparable signal, although with a small difference in chronology. This difference in timing is still within chronological uncertainty. The magnitude of rising $\delta^{18}O$ values in both speleothems after the event is outside the pollen-defined expected range of $\Delta\delta^{18}O_{c\_ptc}$ due to temperature change. Thus, the event likely reflects a change also related to climate–hydrology. The interval coincides with events documented in both archaeological and palaeoclimate records around the eastern Mediterranean (see review in Drake, 2012) that may have led to cultural demise

at the end of the late Bronze Age. Associated with this cold event is a decrease of the Aegean Sea winter surface temperatures, as documented by Rohling et al. (2002). Changes in climate–hydrology are reflected by drought in Cyprus and Syria (Kaniewski et al., 2010, 2013), and a drop of the Dead Sea level (Migowski et al., 2006). In northern Romania, testate amoebae data also indicate a dry phase between 3.4 and 3.0 ka (Schnitchen et al., 2006).

The calculated range of $\Delta\delta^{18}O_{c\_ptc}$ (2.9–2.5 ka to 3.2–2.9 ka) using pollen reconstructed temperatures from Lake Maliq (Bordon et al., 2009) is from -0.13 ‰ for the cold season (reflecting a slight cooling after the event) to 0.27 ‰ for summer season (reflecting a warming). The $\Delta\delta^{18}O_{c\_spel}$ from Ascunsă Cave is 0.4 ‰. This offset (0.13‰ with respect to the upper margin of $\Delta\delta^{18}O_{c\_ptc}$) indicates that changes related to climate–hydrology contributed significantly to the speleothem $\delta^{18}O$ signal. In this case the isotopic evolution out of the 3.2 ka event suggests an increase in summer rainfall or a reduction in winter rain after the 3.2 ka event. The event itself would consequently be characterised by either lower summer rainfall or higher winter rainfall. Higher winter rainfall is not in agreement with widespread drought in the winter rain-dominated eastern Mediterranean. The Mediterranean plays an important role as winter moisture source for southwestern Romania (Bojariu and Paliu, 2001). Consequently, a change in moisture source composition of Mediterranean-derived rainfall could potentially have contributed, but is not observable in Mediterranean foraminifera records (Rohling et al., 2002; Siani et al., 2010). It seems that pollen data from Lake Maliq and marine records from the Mediterranean are not in agreement concerning the timing of temperature change, perhaps due to chronological uncertainty. We note that significant winter cooling is apparent in the abundance record of planktic foraminifera species in the Aegean Sea (Rohling et al., 2002), whereas the Lake Maliq pollen record shows a winter cooling centred between 2.9 and 2.8 ka. Aligning Lake Maliq with the marine chronology would change the sign of $\Delta\delta^{18}O_{c\_spel}$ and $\Delta\delta^{18}O_{c\_pct}$, and the interpretation would be a winter drought for the 3.2 ka event. As such, a change in climate–hydrology is evident for the 3.2 ka event, but cannot currently be defined given chronological uncertainty. However, there is clear evidence for coincidence of a climate event which includes a hydrologic component with a time interval of significant cultural change.

4   Conclusions

The stable isotope record of Ascunsă Cave in southern Romania was used to identify centennial to millennial-scale climate change during the Holocene in this area. By using a novel approach to discriminate between the effects of temperature and hydrology on speleothem $\delta^{18}O$ values, we demonstrate that this shift not only reflects rising regional

temperatures as documented by pollen assemblages (Davis et al., 2003), but also a combination of influences related to changes in climate–hydrology. The approach presented in this study relies on using pollen-based temperature reconstructions to constrain temperature-driven isotopic changes of speleothem calcite. This method considers isotope fractionation occurring during water vapour condensation and calcite precipitation. A constrained range of temperature-driven isotopic changes between winter and summer is obtained, and the deviation of measured data from this range suggests that additional climate–hydrology factors contributed to isotopic variability over the studied period.

Between 6 and 4 ka, δ^{18}O gradually shifted towards higher values in a variety of speleothems across the Mediterranean. Using this approach we find that the middle Holocene enrichment in SW Romania was 0.5–0.6 ‰ greater than values attributable to rising temperatures. A similar situation persists throughout the eastern Mediterranean domain. In the Atlantic-dominated western Romania, as in all parts of the western Mediterranean domain analysed here, changes in δ^{18}O of speleothems largely reflect temperature variations. This reveals a different climate response between the two regions. In the eastern Mediterranean, a combination of higher summer temperatures, enhanced evaporation from the soil and a higher δ^{18}O of the Mediterranean surface water may plausibly explain the observed evolution of δ^{18}O in speleothems across the mid-Holocene.

We also analysed two events of rapid climate change, at 8.2 and 3.2 ka. At Ascunsă Cave, the 8.2 ka event is characterised by a growth rate six times higher than during the rest of the Holocene. The low isotopic variability during the 8.2 ka event seems to reflect mostly temperature variations, but hydrologic conditions such as relatively more summer rainfall at Ascunsă and V11 caves cannot be ruled out. During the 3.2 ka event, both temperature and rainfall seasonality appear to have changed in southern Romania. Data from Ascunsă Cave suggest a significant contribution of changing climate–hydrology, but its nature cannot currently be resolved due to chronological uncertainty in the pollen database.

Appendix A: Calculation method of temperature constrained isotope values

The calculation of the temperature-related part of an observed change in speleothem calcite $\delta^{18}O$ from pollen-based temperature reconstructions relies on two basic assumptions: (1) the cave temperature reflects the annual average surface air temperature and only fluctuates very little around that value (i.e. temperatures in the Ascunsă Cave chamber from which the POM2 stalagmite was collected vary by $0.6\,^\circ C$ over the year); (2) the coldest and warmest month reasonably define the range of temperature-controlled oxygen isotope fractionation during rainfall. This cannot be currently tested for the Ascunsă Cave site due to lack of a continuously recording of stable isotopes in precipitation. However, this assumption is based on information from a large number of European station recordings (Rozanski et al., 1993). In the following, we only consider temperature-related aspects contributing to an observed isotopic change, $\Delta\delta^{18}O$. This has the advantage that accuracy of $\Delta\delta^{18}O$ is determined only by the much less relevant difference of slopes between various water–calcite calibration functions rather than the considerable offsets. For example, the difference in $\Delta\delta^{18}O$ for a temperature change from 10 to $20\,^\circ C$ that would result from using the calibration functions by Kim et al. (2007) and Tremaine et al. (2011), respectively, is only $0.22\,‰$, whereas the difference in absolute $\delta^{18}O$ values is $0.75\,‰$ for $10\,^\circ C$ and $0.97\,‰$ for $20\,^\circ C$ between the two calibration functions.

Generally, $\delta^{18}O$ in calcite ($\delta^{18}O_c$) is determined by the calcification temperature and the isotopic composition of ambient water (Epstein et al., 1953), the latter reflecting rain formation temperature among other hydrologic factors (Rozanski et al., 1993). Consequently, the temperature-related $\Delta\delta^{18}O_c$ can be broken down into $\Delta\delta^{18}O_{ct}$ – the contribution due to changing calcification temperature in the cave – and $\Delta\delta^{18}O_w$ – the contribution due to changing rainfall temperature. The relative change of $\delta^{18}O$ between two time intervals, $t1$ and $t2$, in a speleothem is

$$\Delta\delta^{18}O_{c(t1-t2)} = \Delta\delta^{18}O_{ct(t1-t2)} + \Delta\delta^{18}O_{w(t1-t2)} \tag{A1}$$
$$= \delta^{18}O_{c(t1)} - \delta^{18}O_{c(t2)}.$$

Likewise, the change in pollen temperature anomaly (Davis et al., 2003) is

$$\Delta\mathrm{TA}_{t1-t2}^{\mathrm{pollen}} = \mathrm{TA}_{t1}^{\mathrm{pollen}} - \mathrm{TA}_{t2}^{\mathrm{pollen}}. \tag{A2}$$

The absolute pollen-derived temperature at any given time t is

$$T_t^{\mathrm{pollen}} = T_{\mathrm{today}} + \mathrm{TA}_t^{\mathrm{pollen}}. \tag{A3}$$

The empirically determined fractionation factor α for oxygen isotopes between water and calcite in speleothems is defined as (Tremaine et al., 2011)

$$1000\ln\alpha = 16.1(10^3 T^{-1}) - 24.6. \tag{A4}$$

The fractionation factor is related to measured values for $\delta^{18}O_c$ and $\delta^{18}O_w$ by (e.g. Sharp, 2007)

$$1000\ln(\alpha) \approx \delta^{18}O_c - \delta^{18}O_w, \tag{A5}$$

where we express both $\delta^{18}O$ values in relation to SMOW. Consequently, the right-hand term in Eq. (A4) equals $\delta^{18}O_{ct}$ in the initial definition made for Eq. (A1). In the case of $\delta^{18}O_w = 0$, Eq. (A5) reduces to

$$1000\ln(\alpha) \approx \delta^{18}O_c. \tag{A6}$$

In this case, $\delta^{18}O_c = \delta^{18}O_{ct}$. Although the approximation in Eq. (A6) would deviate somewhat from the true relationship at the given 25–$30\,‰$ difference between the two $\delta^{18}O$ values, most of the error cancels out when calculating

$$\Delta\delta^{18}O_{c(t1-t2)} = \delta^{18}O_{c(t1)} - \delta^{18}O_{c(t2)}. \tag{A7}$$

From Eqs. (A3), (A4), (A6) and (A7) we have

$$\Delta\delta^{18}O_{c(t1-t2)} = 16.1\left(\frac{1}{T_{t1}^{\mathrm{pollen}}} - \frac{1}{T_{t2}^{\mathrm{pollen}}}\right)1000. \tag{A8}$$

To constrain the range of temperature-related variability of $\delta^{18}O_w$ we use the empirical relationship of $0.58\,‰$ $(\delta^{18}O)/\,^\circ C$ for mid-latitudes (Rozanski et al., 1993):

$$\Delta\delta^{18}O_{w(t1-t2)} = 0.58(‰\,^\circ C^{-1})\Delta\mathrm{TA}_{t1-t2}^{\mathrm{p-seasonal}} \tag{A9}$$

with summer (MTWA) and winter (MTCO) temperatures, respectively, from the Davis et al. (2003) pollen-based reconstructions, respectively, for $\Delta\mathrm{TA}^{\mathrm{p-seasonal}}$. Inserting Eqs. (A8) and (A9) into Eq. (A1) yields the pollen temperature-constrained range of change in speleothem calcite ($\Delta\delta^{18}O_{c\_ptc-winter}$ and $\Delta\delta^{18}O_{c\_ptc-summer}$), after conversion to the VPDB scale used for calcite $\delta^{18}O$. This interval constitutes the part of the observed change in the speleothem ($\Delta\delta^{18}O_{c\_spel}$) that may be explained by temperature variability between two defined time intervals (Fig. 8a). Calculations for all cave sites discussed in the main text are summarised in Table 5.

Appendix B: Sources of uncertainty of the calculation

The precision of the pollen-constrained temperature range can in principle be estimated by a full propagation of errors, but these are not generally available for pollen reconstructions. This uncertainty may generally be minimised by averaging reconstructions from many sites, like in Davis et al. (2003). Accuracy will depend on a number of aspects. One is the choice of calcite–water fractionation function (see above). In most cases, however, Holocene temperature changes in Europe rarely exceed $2\,^\circ\text{C}$ (Davis et al., 2003), for which the inaccuracy on $\Delta\delta^{18}O$ as a result of calibration function difference reduces to $\sim 0.05\,$‰ – which is below analytical precision for $\delta^{18}O$ measurements in calcite. Results from Eq. (A9) will also be affected by spatial and temporal variability of the $0.58\,$‰ $(\delta^{18}\text{O}_\text{w})/\,^\circ\text{C}$ slope defined by Rozanski et al. (1993). However, the conclusion that much of the change in $\delta^{18}\text{O}_\text{c\_spel}$ across the 4–6 ka transition in the eastern Mediterranean (Fig. 9) requires a hydrologic component is rather robust against variability of the above slope. The range for calculated temperature-controlled $\Delta\delta^{18}O_{\text{c}-\text{pct}}$ in Fig. 9 would approximately expand twice if the 0.58 slope value were twice as high. However, such variability is not observed in any of the individual stations summarised by Rozanski et al. (1993). This would also not change the main conclusion that the eastern Mediterranean and Balkan region went through a change in climate hydrology that is not observed in the western Mediterranean. The most important aspect is the choice of pollen data sets for the calculation. Here, the question of how representative a respective pollen data set is for the given location of the cave cannot be quantified, but must be justified on the grounds of regional climatology. An example for the impact is the calculation for the Urşilor Cave record (Fig. 9), which is based on a record from a single site, Steregoiu (Feurdean et al., 2008). We chose this site as representative because it is reasonably close to the cave sites, and the Davis et al. (2003) CE quadrant, into whose SW corner the speleothem records would fall is void of any records in this area and thus poorly defined. Had the calculated range of temperature-constrained $\delta^{18}O$ been done using the Davis et al. (2003) record, it would have fallen between -0.1 and $0\,$‰. Consequently, the interpretation for Urşilor would have been the same as with the other Romanian and eastern Mediterranean records. However, the principal east–west gradient across the Mediterranean suggested by our analysis would not change.

References

Alley, R. B., Mayewski, P. A., Sowers, T., Stuiver, M., Taylor, K. C., and Clark, P. U.: Holocene climatic instability: A prominent, widespread event 8,200 years ago, Geology, 25, 483–486, 1997.

Apostol, L.: The Mediterranean cyclones – the role in ensuring water resources and their potential of climatic risk, in the east of Romania, Present Environment and Sustainable Development, 2, 143–163, 2008.

Baltă, D. and Geicu, A.: Factorii dinamici ai atmosferei, In: Clima Românei, edited by: Sandu, I., Pescaru, V. I., Poiană, I., Editura Academiei Române, Bucureşti, 38–51, 2008.

Bar-Matthews, M., Ayalon, A., Matthews, A., Sass, E., and Halicz, L.: Carbon and oxygen isotope study of the active water-carbonate system in a karstic Mediterranean cave: Implications for paleoclimate research in semiarid regions, Geochim. Cosmochim. Ac., 60, 337–347, 1996.

Bar-Matthews, M., Ayalon, A., and Kaufman, A.: Timing and hydrological conditions of Sapropel events in the Eastern Mediterranean, as evident from speleothems, Soreq cave, Israel, Chem. Geol., 169, 145–156, 2000.

Bar-Matthews, M., Ayalon A., Gilmour M., Matthews A., and Hawkesworth C. J.: Sea-land oxygen isotopic relationships from planktonic foraminifera and speleothems in the Eastern Mediterranean region and their implication for paleorainfall during interglacial intervals, Geochim. Cosmochim. Ac., 67, 3181–3199, 2003.

Bojariu, R. and Paliu, D. M.: North Atlantic Oscillation projection on Romanian climate fluctuations in the cold season, In: Detecting and Modelling Regional Climate Change and Associated Impacts, edited by: Brunet, M., and Lopez, D., Springer-Verlag, Berlin, Heidelberg, 345–356, 2001.

Bordon, A., Peyron, O., Lezine, A.-M., Brewer, S., and Fouache, E.: Pollen-inferred Late-Glacial and Holocene climate in southern Balkans (Lake Maliq), Quatern. Int., 200, 19–30, 2009.

Brand, W. A., Geilmann, H., Crosson, E. R., and Rella, C. W.: Cavity ring-down spectroscopy versus high-temperature conversion isotope ratio mass spectrometry; a case study on δ^2H and δ^{18}O of pure water samples and alcohol/water mixtures, Rapid Commun. Mass. Sp., 23, 1879–1884, 2009.

Craig, H.: Isotope variations in meteoric waters, Science, 133, 1702–1703, 1961.

Codarcea, A., Răileanu, G., Năstăseanu, S., Bercia, I., Bercia, E., and Bişioanu, C.: Geological map of Romania, scale 1 : 200 000, L-34-XXIX, Baia de Aramă sheet, Institutul Geologic, Bucureşti, 1964.

Constantin, S., Bojar, A.-V., Lauritzen, S.-E., and Lundberg, J.: Holocene and Late Pleistocene climate in the sub-Mediterranean continental environment: A speleothem record from Poleva Cave Southern Carpathians, Romania, Palaeogeogr. Palaeocl., 243, 322–338, 2007.

Davis, B. A. S., Brewer, S., Stevenson, A., Guiot, J., and Data Contributors: The temperature of Europe during the Holocene reconstructed from pollen data, Quat. Sci. Rev., 22, 1701–1716, 2003.

Day, C. and Henderson, G. M.: Oxygen isotopes in calcite grown under cave-analogue conditions, Geochim. Cosmochim. Ac., 75, 3956–3972, 2011.

Dragotă, C. and Baciu, M.: Cantităiile medii lunare şi anuale de precipita?ii (in Romanian), in: Clima Românei, edited by: Sandu, I., Pescaru, V. I., and Poiană, I., Editura Academiei Române, Bucureiti, 245–264, 2008.

Drake, B. L.: The influence of climatic change on the Late Bronze Age Collapse and the Greek Dark Ages, J. Archaeol. Sci., 39, 1862–1870, 2012.

Drysdale, R., Zanchetta, G., Hellstrom, J., Maas, R., Fallick, A., Pickett, M., Cartwright, I., and Piccini, L.: Late Holocene drought responsible for the collapse of Old World civilizations is recorded in an Italian cave flowstone, Geology, 34, 101–104, 2006.

Enzel, Y., Bookman, R. (Ken Tor), Sharon, D., Gvirtzman, H., Dayan, U., Ziv, B., and Stein, M.: Late Holocene climates of the Near East deduced from Dead Sea level variations and modern regional winter rainfall. Quat. Res., 60, 263–273, 2003.

Epstein, S., Buchsbaum, R., Lowenstamm, H., and Urey, H. C.: Revised carbonate-isotopic temperature scale, Bull. Geol. Soc. Am., 64, 1315–1326, 1953.

Fairchild, I. J., Smith, C. L., Baker, A., Fuller, L., Spötl, C., Mattey, D., McDermott, F., and E. I. M. F.: Modification and preservation of environmental signals in speleothems, Earth-Sci. Rev., 75, 105–153, 2006.

Feurdean, A., Klotz, S., Mosbrugger, V., and Wohlfarth, B.: Pollen-based quantitative reconstructions of Holocene climate variability in NW Romania, Palaeogeogr. Palaeocl., 260, 494–504, 2008.

Fleitmann, D., Cheng, H., Badertscher, S., Edwards, R. L., Mudelsee, M., Göktürk, O. M., Frankhauser, A., Pickering, R., Raible, C. C., Matter, A., Kramers, J., and Tüysüz, O.: Timing and climatic impact of Greenland interstadials recorded in stalagmites from northern Turkey, Geophys. Res. Lett., 36, L19707, doi:10.1029/2009GL040050, 2009.

Frisia, S., Fairchild, I. J., Fohlmeister, J., Miorandi, R., Spötl, C., and Borsato, A.: Carbon mass-balance modelling and carbon

isotope exchange processes in dynamic caves, Geochim. Cosmochim. Ac., 75, 380–400, 2011.

Frogley, R. M., Griffiths, I. H., and Heaton, H. E. T.: Historical biogeography and Late Quat. environmental change of Lake Pamvotis, Ioannina (north-western Greece): evidence from ostracods, J. Biogeogr., 28, 745–756, 2001.

Gat, J. and Carmi, I.: Evolution of the isotopic composition of atmospheric waters in the Mediterranean Sea area, J. Geophys. Res., 75, 3039–3048, 1970.

Hendy, C. H.: The isotopic geochemistry of speleothems I. The calculation of the effects of different modes of formation on the isotopic composition of speleothems and their applicability as palaeoclimatic indicators, Geochim. Cosmochim. Ac., 35, 801–824, 1971.

Hoffmann, D. L.: ^{230}Th isotope measurements of femtogram quantities for U-series dating using multi ion counting MIC MC-ICPMS, Int. J. Mass. Spectrom., 275, 75–79, 2008.

Hoffmann, D. L., Prytulak, J., Richards, D. A., Elliott, T., Coath, C. D., Smart, P. L., and Scholz, D.: Procedures for accurate U and Th isotope measurements by high precision MC-ICPMS, Int. J. Mass. Spectrom., 264, 97–109, 2007.

Kaniewski, D., Paulissen, E., Van Campo, E., Weiss, H., Otto, T., Bretschneider, J., and Van Lerberghe, K.: Late second–early first millennium BC abrupt climate changes in coastal Syria and their possible significance for the history of the Eastern Mediterranean, Quat. Res., 74, 207–215, 2010.

Kaniewski, D., Van Campo, E., Guiot, J., Le Burel, S., Otto, T., and Baeteman, C.: Environmental Roots of the Late Bronze Age Crisis, PLoS ONE 8, e71004, doi:10.1371/journal.pone.007100, 2013.

Kim S.-T. and O'Neil, J. R.: Equilibrium and nonequilibrium oxygen isotope effects in synthetic carbonates, Geochim. Cosmochim. Ac., 61, 3461–3475, 1997.

Kowalczk, A. J. and Froelich, P. N.: Cave air ventilation and CO_2 outgassing by radon-222 modeling: How fast do caves breathe?, Earth Planet. Sc. Lett., 289, 209–219, 2010.

Lachniet, M. S.: Climatic and environmental controls on speleothem oxygen-isotope values, Quat. Sci. Rev., 28, 412–432, 2009.

Leng, M. J., Baneschi, I., Zanchetta, G., Jex, C. N., Wagner, B., and Vogel, H.: Late Quat. palaeoenvironmental reconstruction from Lakes Ohrid and Prespa (Macedonia/Albania border) using stable isotopes, Biogeosciences, 7, 3109–3122, doi:10.5194/bg-7-3109-2010, 2010.

Magny, M., Combourieu-Nebout, N., de Beaulieu, J. L., Bout-Roumazeilles, V., Colombaroli, D., Desprat, S., Francke, A., Joannin, S., Ortu, E., Peyron, O., Revel, M., Sadori, L., Siani, G., Sicre, M. A., Samartin, S., Simonneau, A., Tinner, W., Vannière, B., Wagner, B., Zanchetta, G., Anselmetti, F., Brugiapaglia, E., Chapron, E., Debret, M., Desmet, M., Didier, J., Essallami, L., Galop, D., Gilli, A., Haas, J. N., Kallel, N., Millet, L., Stock, A., Turon, J. L., and Wirth, S.: North–south palaeohydrological contrasts in the central Mediterranean during the Holocene: tentative synthesis and working hypotheses, Clim. Past, 9, 2043–2071, 2013,
http://www.clim-past.net/9/2043/2013/.

Magyari, E., Buczkó, K., Jakab, G., Braun, M., Pál, Z., Karátson, D., and Pap, I.: Palaeolimnology of the last crater lake in the Eastern Carpathian Mountains: a multiproxy study of Holocene hy-

drological changes, Palaeolimnological Proxies as Tools of Environmental Reconstruction in Fresh Water, Develop. Hydrobiol., 208, 29–63, 2009.

Marino, G., Rohling, E. J., Sangiorgi, F., Hayes, A., Casford, J. L., Lotter, A. F., Kucera, M., and Brinkhuis, H.: Early and middle Holocene in the Aegean Sea: interplay between high and low latitude climate variability, Quat. Sci. Rev., 28, 3246–3262, 2009.

Mayewski, P. A., Rohling, E., Stager, J. C., Karlén, W., Maasch, K. A., Meeker, L. D., Meyerson, E. A., Gasse, F., van Kreveld, S., Holmgren, K., Lee-Thorp, J., Rosqvist, G., Rack, F., Staubwasser, M., Schneider, R. R., and Steig, E. J.: Holocene climate variability, Quat. Res., 62, 243–255, 2004.

McDermott, F., Frisia, S., Huang, Y., Longinelli, A., Spiro, B., Heaton, T. H. E., Hawkesworth, C. J., Borsato, A., Keppens, E., Fairchild, I. J., van der Borg, K., Verheyden, S., and Selmo, E.: Holocene climate variability in Europe: Evidence from δ^{18}O, textural and extension-rate variations in three speleothems, Quat. Sci. Rev., 18, 1021–1038, 1999.

McDermott, F.: Palaeo-climate reconstruction from stable isotope variations in speleothems: a review, Quat. Sci. Rev., 23, 901–918, 2004.

McDermott, F., Atkinson, T. C., Fairchild, I. J., Baldini, L. M., and Mattey, D. P.: A first evaluation of the spatial gradients in δ^{18}O recorded by European Holocene speleothems, Global Planet. Change, 79, 275–287, 2011.

Migowski, C., Stein, M., Prasad, S., Negendank, J. F. W., and Agnon, A.: Holocene climate variability and cultural evolution in the Near East from the Dead Sea sedimentary record, Quat. Res., 66, 421–431, 2006.

Onac, B. P., Constantin, S., Lundberg, J., and Lauritzen S.-E.: Isotopic climate record in a Holocene stalagmite from Urşilor Cave Romania, J. Quat. Sci., 17, 319-327, 2002.

Panagiotopoulos, K., Aufgebauer, A., Schäbitz, F., and Wagner, B.: Vegetation and climate history of the Lake Prespa region since the Lateglacia, Quatern. Int., 293, 157–169, 2013.

Pross, J., Kotthoff, U., Müller, U. C., Peyron, O., Dormoy, I., Schmiedl, G., Kalaitzidis, S., and Smith, A. M.: Massive perturbation in terrestrial ecosystems of the Eastern Mediterranean region associated with the 8.2 kyr B. P. climatic event, Geology, 37, 887–890, 2009.

Riechelmann, D. F. C., Deininger, M., Scholz, D., Riechelmann, S., Schröder-Ritzrau, A., Spötl, C., Richter, D. K., Mangini, A., and Immenhauser, A.: Disequilibrium carbon and oxygen isotope fractionation in recent cave calcite: Comparison of cave precipitates and model data, Geochim. Cosmochim. Ac. 103, 232–244, 2013.

Roberts, N., Jones, M. D., Benkaddour, A., Eastwood, W. J., Filippi, M. L., Frogley, M. R., Lamb, H. F., Leng, M. J., Reed, J. M., Stein, M., Stevens, L., Valero-Garcés, B., and Zanchetta, G.: Stable isotope records of Late Quat. climate and hydrology from Mediterranean lakes: the ISOMED synthesis, Quat. Sci. Rev., 27, 2426–2441, 2008.

Roberts, N., Eastwood, W. J., Kuzucuoğlu, C., Fiorentino, G., and Caracuta V.: Climatic, vegetation and cultural change in the eastern Mediterranean during the mid-Holocene environmental transition, Holocene, 21, 147–162, 2011.

Rodwell, M. J. and Hoskins, B. J.: Monsoons and the dynamics of deserts, Q. J. Roy. Meteor. Soc., 122, 1385–1404, 1996.

Rohling, E. J. and Pälike, H.: Centennial-scale climate cooling with a sudden cold event around 8,200 years ago, Nature, 434, 975–979, 2005.

Rohling, E. J., Mayewski, P. A., Abu-Zied, R. H., Casford, J. S. L., and Hayes, A.: Holocene atmosphere-ocean interactions: records from Greenland and the Aegean Sea, Clim. Dynam., 18, 587–593, 2002.

Rossignol-Strick, M.: The Holocene climatic optimum and pollen records of sapropel 1 in the eastern Mediterranean, 9000–6000 BP, Quat. Sci. Rev., 18, 515–530, 1999.

Rozanski, K., Sonntag C., and Münnich K. O.: Factors controlling stable isotope composition of modern European precipitation, Tellus, 34, 142–150, 1982.

Rozanski, K., Araguás-Araguás, L., and Gonfiantini, R.: Isotopic patterns in modern global precipitation, In: Climate change in continental isotopic records (eds: Swart, P. K., Lohmann, K. C., McKenzie, J., and Savin, S.), Geoph. Monog. Series, 78, 1–36, 1993.

Schnitchen, C., Charman, D. J., Magyari, E., Braun, M., Grigorszky, I., Tóthmérész, B., Molnár, M., and Szántó, Z.: Reconstructing hydrological variability from testate amoebae analysis in Carpathian peatlands, J. Paleolimnol., 36, 1–17, 2006.

Scholz, D. and Hoffmann, D. L.: StalAge: An algorithm designed for construction of speleothem age models, Quat. Geochronol., 6, 369–382, 2011.

Scholz, D., Frisia, S., Borsato, A., Spötl, C., Fohlmeister, J., Mudelsee, M., Miorandi, R., and Mangini, A.: Holocene climate variability in north-eastern Italy: potential influence of the NAO and solar activity recorded by speleothem data, Clim. Past, 8, 1367–1383, 2012,
http://www.clim-past.net/8/1367/2012/.

Sharp, Z.: Principles of stable isotope geochemistry, Pearson Education Inc., pp344, Upper Saddle River, 2007.

Siani, G., Paterne, M., and Colin, C.: Late glacial to Holocene planktic foraminifera bioevents and climatic record in the South Adriatic Sea, J. Quat. Sci., 25, 808–821, 2010.

Spötl, C., Fairchild, I. J., and Tooth, A.: Cave air control on dripwater geochemistry, Obir Caves (Austria): Implications for speleothem deposition in dynamically ventilated caves, Geochim. Cosmochim. Ac., 69, 2451–2468, 2005.

Staubwasser, M., and Weiss, H.: Holocene climate and cultural evolution in late prehistoric-early historic West Asia – Introduction, Quat. Res., 66, 372–387, 2006.

Tămaş, T., Onac, B. P., and Bojar, A.-V.: Lateglacial-Middle Holocene stable isotope records in two coeval stalagmites from the Bihor Mountains, NW Romania, Geol. Q., 49, 185–194, 2005.

Tremaine, D. M., Froelich, and P. N., Wang. Y.: Speleothem calcite farmed in situ: Modern calibration of δ^{18}O and δ^{13}C paleoclimate proxies in a continuously-monitored natural cave system, Geochim. Cosmochim. Ac., 75, 4929–4950, 2011.

Trigo, I. F., Bigg, G. R., and Davies, T. D.: Climatology of cyclogenesis mechanisms in the Mediterranean, Mon. Weather Rev., 130, 549–569, 2002.

Verheyden, S., Nader, F., Cheng, H., Edwards, L., and Swennen, R.: Paleoclimate reconstruction in the Levant region from the geochemistry of a Holocene stalagmite from the Jeita cave, Lebanon, Quat. Res., 70, 368–381, 2008.

Vollweiler, N., Scholz, D., Mühlinghaus, C., Mangini, A., and Spötl, C.: A precisely dated climate record for the last 9 kyr from three high alpine stalagmites, Spannagel Cave, Austria, Geophys. Res. Lett., 33, L20703, doi:10.1029/2006GL027662, 2006.

Wanner, H., Beer, J., Bütikofer, J., Crowley, T. J., Cubasch, U., Flückiger, J., Goosse, H., Grosjean, M., Joos, F., Kaplan, J. O., Küttel, M. l., Müller, S. A., Prentice, I. C., Solomina, O., Stocker, T. F., Tarasov, P., Wagner, M., and Widmann, M.: Mid- to Late Holocene climate change: an overview, Quat. Sci. Rev., 27, 1791–1828, 2008.

Wanner, H., Solomina, O., Grosjean, M., Ritz, S. P., and Jetel, M.: Structure and origin of Holocene cold events, Quat. Sci. Rev., 30, 3109–3123, 2011.

Wedepohl, H. K.: The composition of the continental crust, Geochim. Cosmochim. Ac., 59, 1217–1232, 1995.